Arch Biol Sci. 2025;77(3):209-224 https://doi.org/10.2298/ABS250429017X

Caffeic acid phenethyl ester as a potent adjuvant: augmenting cisplatin's antitumor activity while mitigating nephrotoxicity in triple-negative breast cancer

Luyi Xi[1], Yuyue Yao[1], Ying Lu[1], Hongtao Hu[1], and Huajun Zhao[1,2,*]

[1]*School of Pharmaceutical Sciences, Zhejiang Chinese Medical University*, Hangzhou 311402, China
[2]*Academy of Chinese Medical Sciences, Zhejiang Chinese Medical University*, Hangzhou 310053, China

***Corresponding author**: zhj@zcmu.edu.cn

Received: April 29, 2025; **Revised**: June 9, 2025; **Accepted**: June 15, 2025; **Published online**: June 23, 2025

Abstract: Triple-negative breast cancer (TNBC) remains a significant clinical challenge due to its aggressive nature and limited treatment options. Cisplatin is a widely used chemotherapeutic agent for TNBC, but its clinical application is hindered by dose-limiting nephrotoxicity. Caffeic acid phenethyl ester (CAPE), a bioactive component of propolis with known antitumor and organ-protective effects, has potential as an adjuvant to chemotherapy. This study evaluates the synergistic antitumor efficacy of CAPE combined with cisplatin and its ability to mitigate nephrotoxicity. *In vitro*, the CAPE-cisplatin combination synergistically inhibited TNBC cell proliferation, an effect reversed by the apoptosis inhibitor Z-VAD-FMK and the ROS scavenger N-acetylcysteine. Enhanced apoptosis was confirmed by Annexin V/PI staining and elevated cleaved caspase-3 levels, while increased ROS generation was verified by DCFH-DA flow cytometry. DNA damage was further supported by comet assays, immunofluorescence, immunocytochemistry, and Western blotting. Mechanistic studies using network pharmacology, transcriptomics, and Western blotting implicated the MAPK signaling pathway in mediating the therapeutic synergy. *In vivo*, combination therapy significantly enhanced the antitumor efficacy of a subtherapeutic dose of cisplatin and reduced nephrotoxicity compared to monotherapies. These findings suggest that CAPE potentiates the anticancer effects of cisplatin in TNBC while providing renal protection, offering a promising strategy to improve chemotherapy outcomes with reduced toxicity.

Keywords: synergistic antitumor, caffeic acid phenethyl ester, cisplatin, triple-negative breast cancer, MAPK signaling pathway.

Abbreviations: CAPE – caffeic acid phenethyl ester; ALT – alanine aminotransferase; AST – aspartate aminotransferase; TNBC – triple-negative breast cancer; CI – Combination Index; DAPI – 4′, 6-diamidino-2-phenylindole; DMSO – dimethyl sulfoxide; H&E – hematoxylin & eosin staining; IHC – immunohistochemistry; MAPK – mitogen-activated protein kinase; MTT – 3-4,5-dimethylthiazol-2-yl-2,5-diphenyltetrazolium bromide

INTRODUCTION

As one of the most prevalent malignant tumors, breast cancer ranks first in incidence and second in mortality among female cancers [1, 2]. Triple-negative breast cancer (TNBC), characterized by the absence of estrogen receptors (ER), progesterone receptors (PR), and human epidermal growth factor receptor 2 (HER2), represents approximately 15% of all breast cancer cases [3]. This subtype is characterized by its particularly aggressive behavior, high malignancy, recurrence tendency, and significant metastatic potential [4]. The rate of TNBC recurrence is up to 25% and the median survival time is less than 2 years [5, 6]. Therefore, the treatment of patients with TNBC remains a huge challenge.

The primary treatment for TNBC relies on chemotherapy, including anthracyclines, paclitaxel, and platinum drugs [7]. Among them, cisplatin, a DNA-damaging agent, demonstrates robust antitumor activity by causing cross-linking and DNA breakage in cancers. This therapeutic effect is amplified in TNBC due to characteristic deficiencies in DNA damage repair [8, 9]. A research team from the Affiliated Cancer Hospital of

Fudan University has demonstrated the effectiveness of cisplatin in patients with metastatic TNBC and explored the potential of combining cisplatin with different chemotherapeutic agents to further augment therapeutic outcomes [10]. However, the nephrotoxicity of cisplatin frequently leads to reduced treatment adherence and diminished quality of life in cancer patients, posing a major challenge to long-term therapeutic efficacy [11]. Current mitigation strategies, including hydration regimens, diuretics, and antioxidants, demonstrate suboptimal efficacy, underscoring the importance for innovative therapeutic approaches [12]. Therefore, there is an urgent need to explore combination therapies that can enhance the therapeutic efficacy of chemotherapy while mitigating nephrotoxicity.

Given the limitations of platinum-based therapy, natural compounds with synergistic potential have gained much attention. Traditional Chinese medicine (TCM), with a millennia-old heritage in China, offers distinctive therapeutic advantages including multi-targets, lower adverse reactions, and enhancement of the immune system through holistic regulation [13]. Thus, combining cisplatin with natural compounds may provide a more effective therapy [14]. Propolis, a resinous substance produced by honeybees through the combination of glandular secretions and plant resins, demonstrates significant antitumor properties and serves as a clinically recognized adjuvant in cancer therapy [15]. Caffeic acid phenethyl ester (CAPE), the predominant phenolic acid constituent in propolis, serves as a key quality control marker for propolis products. Wu et al. reported that CAPE demonstrated a variety of antitumor effects, including promoting apoptosis, modulating the cell cycle, and inhibiting angiogenesis, without any noticeable impact on normal mammary cells [16]. Then Colombo et al. demonstrated its capacity to enhance the sensitivity of cisplatin in cisplatin-resistant ovarian tumors by regulating the ubiquitin-specific protease 8 (USP8) [17]. Accumulating evidence has well-documented the multi-organ protective effects of CAPE against chemotherapy-induced toxicity. In particular, CAPE has been shown to effectively alleviate doxorubicin-induced cardiotoxicity and tamoxifen-induced hepatotoxicity in preclinical studies [18-20]. Moreover, previous studies have demonstrated that CAPE exhibited nephroprotective effects in healthy animal models against high-dose cisplatin-induced renal damage through antioxidant pathways [21]. However, its renoprotective potential in tumor-bearing models receiving chronic low-dose cisplatin remains unclear. A critical question remains whether CAPE can preserve renal function without attenuating cisplatin's antitumor activity, which constitutes a key focus of the present investigation.

In this study, a thorough investigation of the potential synergistic effects of CAPE and cisplatin on TNBC was conducted both *in vitro* and *in vivo*. Our results show that this combination therapy has a favorable synergistic antitumor effect on TNBC by regulating the MAPK pathway without causing nephrotoxicity.

MATERIALS AND METHODS

Ethics statement

Animal experiments were approved by the Institutional Animal Care and Use Committee of Zhejiang Chinese Medical University (Approval No.: PHA-IACUC-20241028-02) and carried out in accordance with the guidelines of the Laboratory Animal Research Center of Zhejiang Chinese Medical University.

Materials

Caffeic acid phenethyl ester (CAPE, #HY-N0274) was purchased from MedChemExpress (NJ, USA). Cisplatin (cisplatin, #15663-27-1) was obtained from Shanghai yuanye Bio-Technology Co. Ltd (Shanghai, China). Antibodies against p-ERK (#9101), ERK (#9102), p-p38 (4511s), p38 MAPK(#8690S), p-JNK (#4668), and JNK (#3708) were obtained from Cell Signaling Technology (MA, USA). Antibody against GAPDH (#E12-042-3) was acquired from EnoGene (Nanjing, China), the antibody against γ-H2AX was purchased from Abcam (Cambridge, UK). ALT (#C009-2-1) and AST (#C010-2-1) kits were purchased from Jiancheng (Nanjing, China).

Cell lines and cell culture

The human TNBC cell line MDA-MB-468 and mouse TNBC cell line 4T1 were obtained from the Chinese Academy of Sciences (Shanghai, China). All cells were cultured with DMEM/F12 medium (Gibco, Grand Island, NY, USA), supplemented with 10% FBS (Gibco,

Grand Island, NY, USA) in a humidified incubator at 37°C with 5% CO_2, and passaged every 3 days.

Cell viability assay

Logarithmic TNBC cells were seeded into 96-well plates at a density of 5×10^3 cells per well and exposed to CAPE and cisplatin for 48 h after cell adhesion. MTT (Gibco, Grand Island, NY, USA) solution (5 mg/mL) was added to each well and DMSO (Gibco, Grand Island, NY, USA) was added to dissolve the formazan crystals after 4 h. Then absorbance was measured at 490 nm.

Calculation of the combination index

Drug synergy was evaluated and analyzed with CompuSyn software (Biosoft, Ferguson, MO, USA). The combination index (CI)<1 indicates synergistic effects.

Colony formation assay

Cells were seeded into a 12-well plate at a density of 1×10^3 cells per well and cultured in a medium containing CAPE and cisplatin. Following seeding, plates were incubated in a humidified atmosphere of 5% CO_2 at 37°C for 14 days. After the incubation, the culture medium was carefully aspirated, and cells were fixed with 4% paraformaldehyde solution for 15 min at room temperature. Fixed cells were then stained with 0.1% (w/v) crystal violet solution for 15 min in the dark. Following staining, wells were gently rinsed three times with phosphate-buffered saline (PBS) to remove excess dye and air-dried overnight at room temperature before acquiring images.

Measurement of ROS production

Cells were seeded into 6-well plates and harvested after incubating with culture medium containing drugs for 24 h. They were then dyed with DCFH-DA for 30 min at 37°C in the dark and analyzed by flow cytometer.

Cell apoptosis

Cells were seeded into 6-well plates and collected after exposure to drugs for 48 h. According to the instructions of the cell apoptosis kit (Beyotime, Shanghai, China), cells were washed with PBS and then stained with Annexin V-FITC and PI for 15 min at 25°C in the dark. After being resuspended with binding buffer, cells were analyzed by flow cytometry.

Comet assay

As described previously [22], cells were treated with drugs for 24 h, harvested, mixed with 0.6% low-melting agarose, spread on 0.6% normal-melting point agarose, and left at 4°C for 10 min to solidify. The gel was lysed in alkaline lysis buffer at 4°C for 1.5 h, and then electrophoresis was performed at 300 V for 20 min. After the pH was neutralized with 0.4 M Tris-HCl, the samples were dehydrated with 50%, 75%, and 100% ethanol for 5 min and dried naturally overnight. Samples were dyed with Gel-Red in the dark, and images were captured within 24 h. Images were imported into ImageJ and analyzed with the OpenComet plugin.

Immunofluorescence staining

Cells were seeded into 24-well plates at a density of 1×10^4 per well, then the culture medium was removed and fixed with 4% paraformaldehyde after being treated with drugs for 24 h. Sequentially, they were permeabilized with 0.5% Triton X-100 for 1 h and blocked with 1% bovine serum albumin (BSA) for 1 h. Followed by incubation with the antibody of γ-H2AX overnight, cells were incubated with Texas Red-labeled goat anti-rabbit IgG Ab for 2 h at room temperature, and then stained with the fluorescent stain 4′,6-diamidino-2-phenylindole (DAPI) for 10 min. Finally, images were captured using a fluorescence microscope (Carl Zeiss, China).

Western blotting analysis

Western blotting was performed as described previously [23]. Proteins were extracted using RIPA lysis buffer, and concentrations were determined using the bicinchoninic acid (BCA) assay. Equal amounts of protein samples were separated by sodium dodecyl sulfate-polyacrylamide gel electrophoresis (SDS-PAGE) and then transferred to polyvinylidene fluoride or polyvinylidene difluoride (PVDF) membranes. The membranes were blocked with 5% skim milk, incubated

with primary antibodies, followed by incubation with secondary antibodies. Protein bands were visualized using an enhanced chemiluminescence (ECL) detection system (Bio-Rad Laboratories, Inc. USA).

In vivo tumor model

Female BALB/c nude mice (4-6 weeks old) were provided by Hangzhou Qizhen Experimental Animal Technology Co., Ltd. (Hangzhou, China). A total of 2×10^6 of 4T1 cells were injected into the dorsal flank of each mouse. After a week, they were randomly divided into 4 groups: control, cisplatin (1 mg/kg), CAPE (10 mg/kg), and cisplatin (1 mg/kg) + CAPE (10 mg/kg). Cisplatin was administered intraperitoneally every three days and CAPE was administered intraperitoneally once a day. Body weight was measured every other day, and tumor size was calculated with the formula:

$$\text{volume} = (\text{width}^2 \times \text{length}) \div 2 \quad (1)$$

After 2 weeks, blood, liver, and kidney were harvested for further studies.

Liver and kidney index

Liver and kidney indices were calculated as:

$$\text{Index} = \text{organ weight (mg)} \div \text{body weight(g)} \quad (2)$$

H&E staining and IHC analysis

Tissue was fixed with formalin and embedded in paraffin. Slices were incubated with γ-H2AX for IHC staining or stained with H&E for histological analysis.

Transcriptomics analysis

MDA-MB-468 cells were inoculated in 6-well plates, and the cells were collected after treatment with cisplatin and CAPE for 24 h. The samples were washed with PBS, resuspended, and centrifuged at 1,000 × g for 5 min. After supernatant removal, 200 μL of TRIzol lysate was added for cell lysis, and the lysate was stored on dry ice. Then the samples were sent to Beijing Tsingke Biotech Co., Ltd. for transcriptomics analysis.

Network pharmacology

The chemical structures of cisplatin and CAPE were obtained from PubChem (https://pubchem.ncbi.nlm.nih.gov/) and saved in SMILES format. Potential targets of cisplatin and CAPE were predicted using SuperPRED (https://prediction.charite.dep) [23, 24]. The above targets were unified into official gene symbols using Uniprot (https://www.uniprot.org/). The online Venn diagram tool (https://bioinfogp.cnb.csic.es/tools/venny/) was used to obtain the targets of cisplatin and CAPE. Enrichment analysis was performed using Metascape (https://metascape.org/gp/index.html).

Statistical analysis

The results of the experiments were analyzed by GraphPad Prism 8.3. All data were expressed as the mean±SD. The comparisons of stats between groups were performed by Student's t-test.

RESULTS

CAPE combined with cisplatin synergistically inhibits the growth of TNBC cells

The cytotoxicity of CAPE on TNBC cells was first assessed using the MTT assay at concentrations ranging from 1.875 to 60 μM for 48 h. Notably, CAPE dose-dependently inhibited the growth of MDA-MB-468 and 4T1 cells, and 4T1 cells (IC_{50}=3.03±0.64 μM) were more sensitive to CAPE than MDA-MB-468 cells (IC_{50}=26.31±1.53 μM) (Fig. 1A, B). Based on this, the synergistic antitumor effects of CAPE with various concentrations of cisplatin were investigated and analyzed by CompuSyn software. The combination of CAPE and cisplatin showed synergistic antiproliferative effects, as evidenced by CI values consistently below 1 (Fig. 1C-H). Considering the inhibitory effect and CI values, 2 μM of cisplatin was used to combine with 7.5 μM of CAPE for subsequent experiments in MDA-MB-468 cells, and 2.5 μM of cisplatin with 7.5 μM of CAPE was chosen in 4T1 cells. Colony formation analysis also found that CAPE combined with cisplatin exhibited significant antitumor effects compared with monotherapy (Fig. 1I). These findings suggest that the combination of CAPE and cisplatin has synergistic inhibitory effects on TNBC cells.

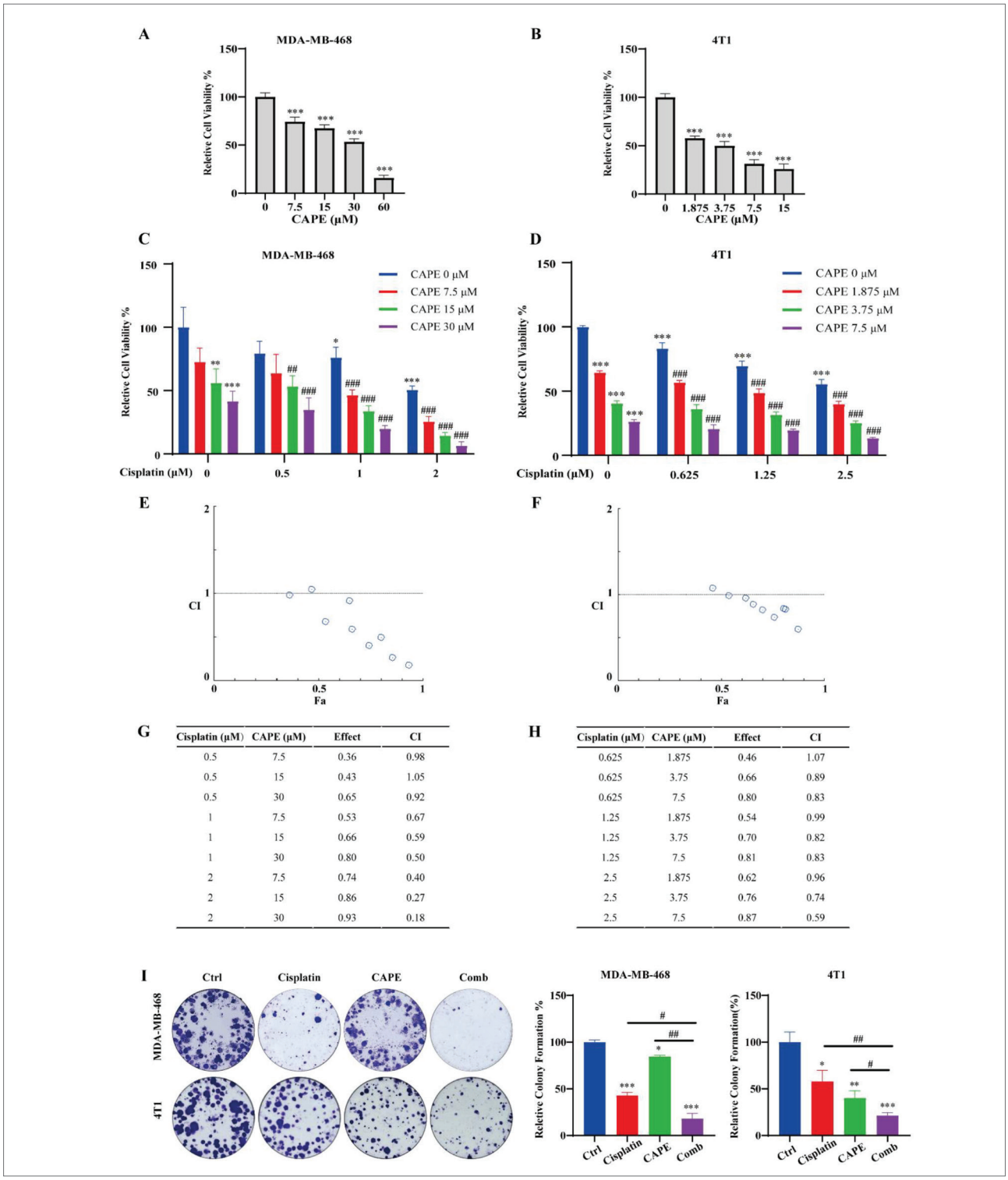

G

Cisplatin (μM)	CAPE (μM)	Effect	CI
0.5	7.5	0.36	0.98
0.5	15	0.43	1.05
0.5	30	0.65	0.92
1	7.5	0.53	0.67
1	15	0.66	0.59
1	30	0.80	0.50
2	7.5	0.74	0.40
2	15	0.86	0.27
2	30	0.93	0.18

H

Cisplatin (μM)	CAPE (μM)	Effect	CI
0.625	1.875	0.46	1.07
0.625	3.75	0.66	0.89
0.625	7.5	0.80	0.83
1.25	1.875	0.54	0.99
1.25	3.75	0.70	0.82
1.25	7.5	0.81	0.83
2.5	1.875	0.62	0.96
2.5	3.75	0.76	0.74
2.5	7.5	0.87	0.59

Fig. 1. CAPE combined with cisplatin synergistically inhibits the growth of TNBC cells. **AB** – After MDA-MB-468 and 4T1 cells were treated with CAPE for 48 h, the cell viability was detected by MTT assay. **CD** – After MDA-MB-468 and 4T1 cells were treated with cisplatin and CAPE for 48 h, the cell viability was detected by MTT assay. **E-H** – CI values were calculated to estimate the synergistic effect of this combination. **I** – After MDA-MB-468 and 4T1 cells were treated with cisplatin and CAPE for 2 weeks, the colony formation was stained by crystal violet solution. Data are presented as the mean±SD. *P<0.05, **P<0.01 and ***P<0.001 vs control group; $^{\#}$P<0.05, $^{\#\#}$P<0.01 and $^{\#\#\#}$P<0.001 vs the combination group.

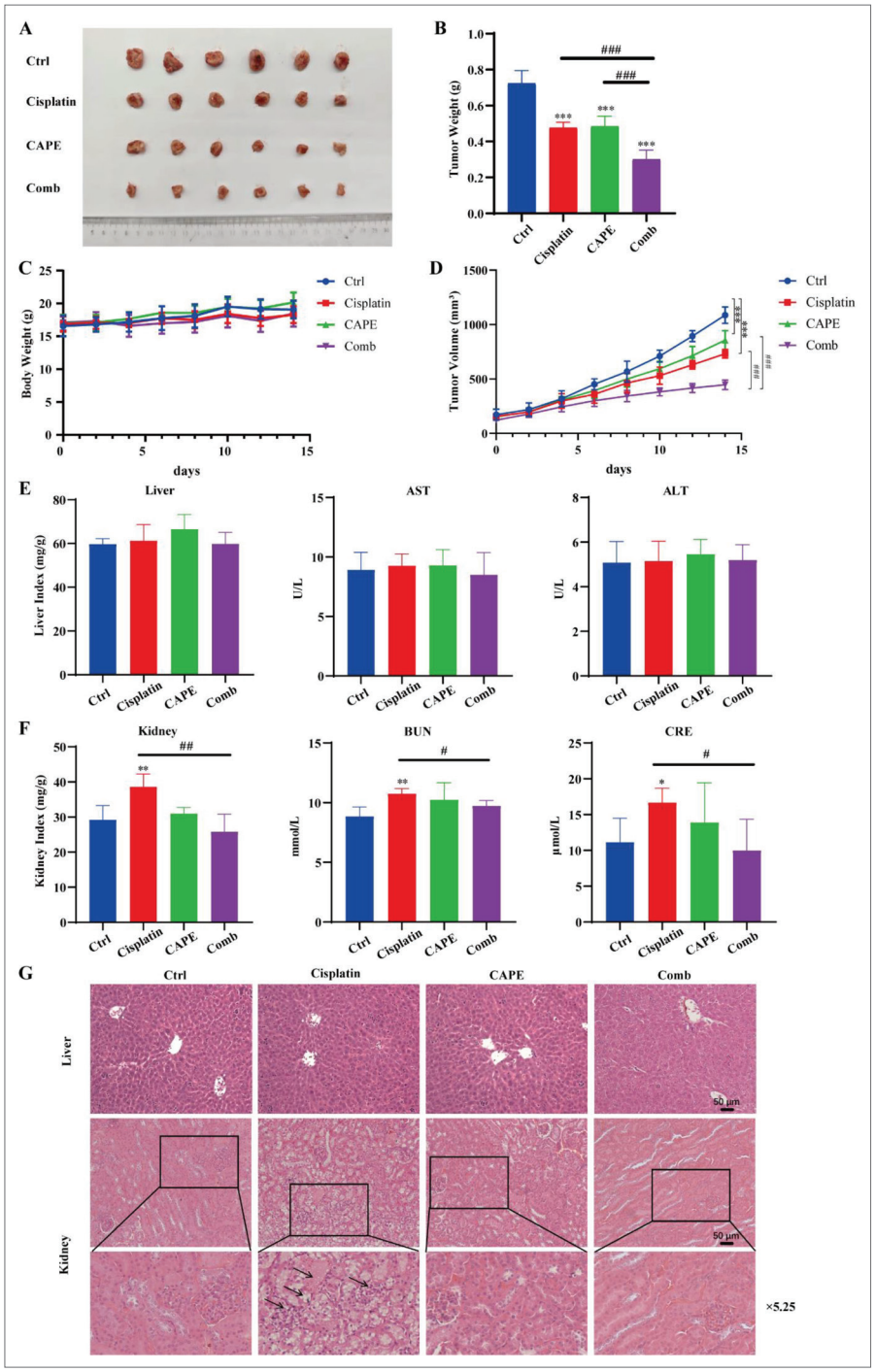

Fig. 2. The co-treatment of cisplatin and CAPE inhibits TNBC growth *in vivo*. **A** – Representative images of tumors. **B** – Tumor weight, **C** – body weight, and **D** – tumor volume were measured. **E** – Calculation of liver index and determination of AST and ALT in serum of each group of mice. **F** – Calculation of kidney index and determination of BUN and CRE in serum of each group of mice. **G** – Representative H&E staining of liver and kidney sections from each group of mice. The black arrows indicate localized necrosis, glomerular atrophy, and vacuolization induced by cisplatin in renal tissue. Data are presented as the mean ± SD. *P<0.05, **P<0.01 and ***P<0.001 vs control group; $^{\#}$P<0.05, $^{\#\#}$P<0.01 and $^{\#\#\#}$P<0.001 vs combination group.

CAPE combined with cisplatin significantly inhibits TNBC tumor growth *in vivo*

To further assess the antitumor effects of CAPE combined with cisplatin, the *in vivo* TNBC model was established. Consistent with the above results, co-treatment of CAPE (10 mg/kg) and cisplatin (1 mg/kg) also exhibited significant tumor growth suppression compared with monotherapy, without obvious body weight loss and liver damage (Fig. 2A-E and 2G). Interestingly, 1 mg/kg cisplatin exhibited significant kidney toxicity with increased levels of the kidney index, blood urea nitrogen (BUN), and creatinine (CRE), whereas CAPE decreased these levels and exerted a protective effect on the kidney (Fig. 2F). H&E staining revealed that cisplatin induced pathological alterations in renal tissue, including localized necrosis, glomerular atrophy, and vacuolization. However, these alterations were significantly attenuated by CAPE's co-treatment with cisplatin (Fig. 2G). These findings suggest that the combination of CAPE and low-dose cisplatin not only significantly inhibits tumor growth but also has a protective effect on the kidneys.

Co-treatment of CAPE and cisplatin induces apoptosis and ROS overproduction in TNBC cells

To elucidate the ways of CAPE and cisplatin induced-cell death, inhibitors of ROS (acetylcysteine, NAC), apoptosis (Z-VAD-FMK), autophagy (chloroquine, CQ), pyroptosis (disulfiram, DSF), necroptosis (necrostatin-1, Nec-1), and ferroptosis (ferrostatin-1, Fer-1; deferoxamine, DFO) were used in 4T1 and

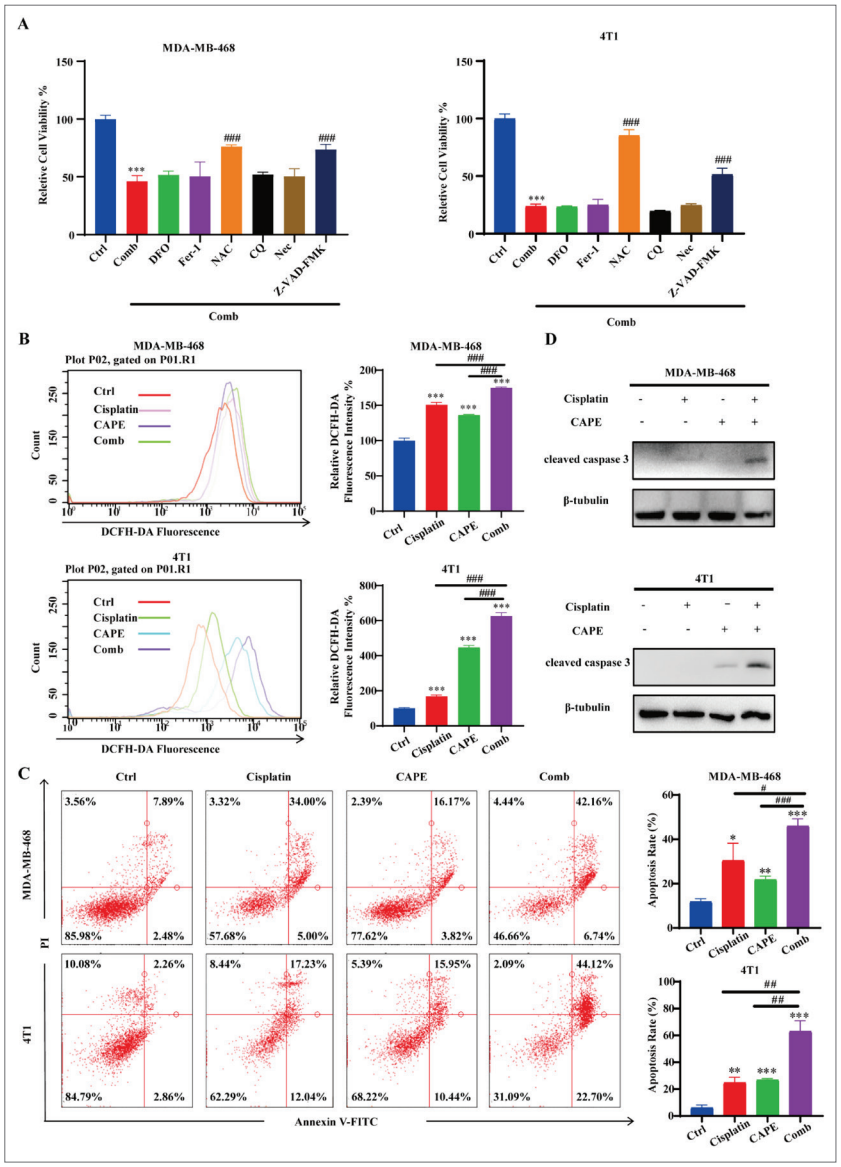

Fig. 3. The co-treatment of cisplatin and CAPE induces cell apoptosis and ROS overproduction in TNBC cells. **A** – MDA-MB-468 and 4T1 cells were treated with different inhibitors for 36 h, followed by MTT analysis for cell viability. **B** – Cells were stained with DCFH-DA and analyzed for fluorescence by flow cytometry. **C** – After Annexin V-FITC/PI staining, the index of apoptotic cells was analyzed by flow cytometry. **D** – The expression levels of cleaved caspase 3 of each group were detected by Western blotting. Data are presented as the mean ± SD. *P<0.05, **P<0.01 and ***P<0.001 vs control group; $^{\#}$P<0.05, $^{\#\#}$P<0.01 and $^{\#\#\#}$P<0.001 vs combination group.

MDA-MB-468 cells. Notably, cell viability was restored by Z-VAD-FMK and NAC (Fig. 3A). Flow cytometry revealed that the combination of CAPE and cisplatin markedly enhanced ROS accumulation and apoptosis (Fig. 3B and C), aligning with the MTT assay results. Similarly, cleaved caspase 3, known as a marker of apoptosis [25, 26], was significantly upregulated compared with CAPE or cisplatin alone (Fig. 3D). These findings suggest that co-treatment of CAPE and cisplatin induces apoptosis and ROS overproduction in TNBC cells.

CAPE enhances DNA damage induced by cisplatin

As a DNA damage agent, cisplatin obstructs the normal progression of DNA replication by forming interstrand crosslinks (ICLs) with DNA and eliciting DNA double-strand breaks (DSBs). To further investigate whether CAPE enhances cisplatin-induced DNA damage, the comet assay was conducted in MDA-MB-468 and 4T1 cells. The results showed that CAPE significantly enhanced cisplatin-induced DNA damage (Fig. 4A and B). As a marker of DNA double-strand breaks and damage, γ-H2AX (Ser-139) is a kind of checkpoint protein that initiates a homologous recombination repair system after cisplatin-induced DNA damage [27]. As shown in Fig. 4C-D, co-treatment of cisplatin and CAPE markedly increased the expression of γ-H2AX, which was further confirmed by immunohistochemistry analysis *in vivo* (Fig. 4E). These findings indicate that CAPE enhances DNA damage induced by cisplatin.

ROS overproduction contributes to DNA damage and apoptosis induced by a combination of cisplatin and CAPE

Evidence from the literature suggests that ROS could induce DNA damage and apoptosis, which can be inhibited by oxygen radical scavengers such as NAC [28, 29]. Consistent with these findings, our results demonstrated that apoptosis was almost completely inhibited and the remarkable accumulation of γ-H2AX

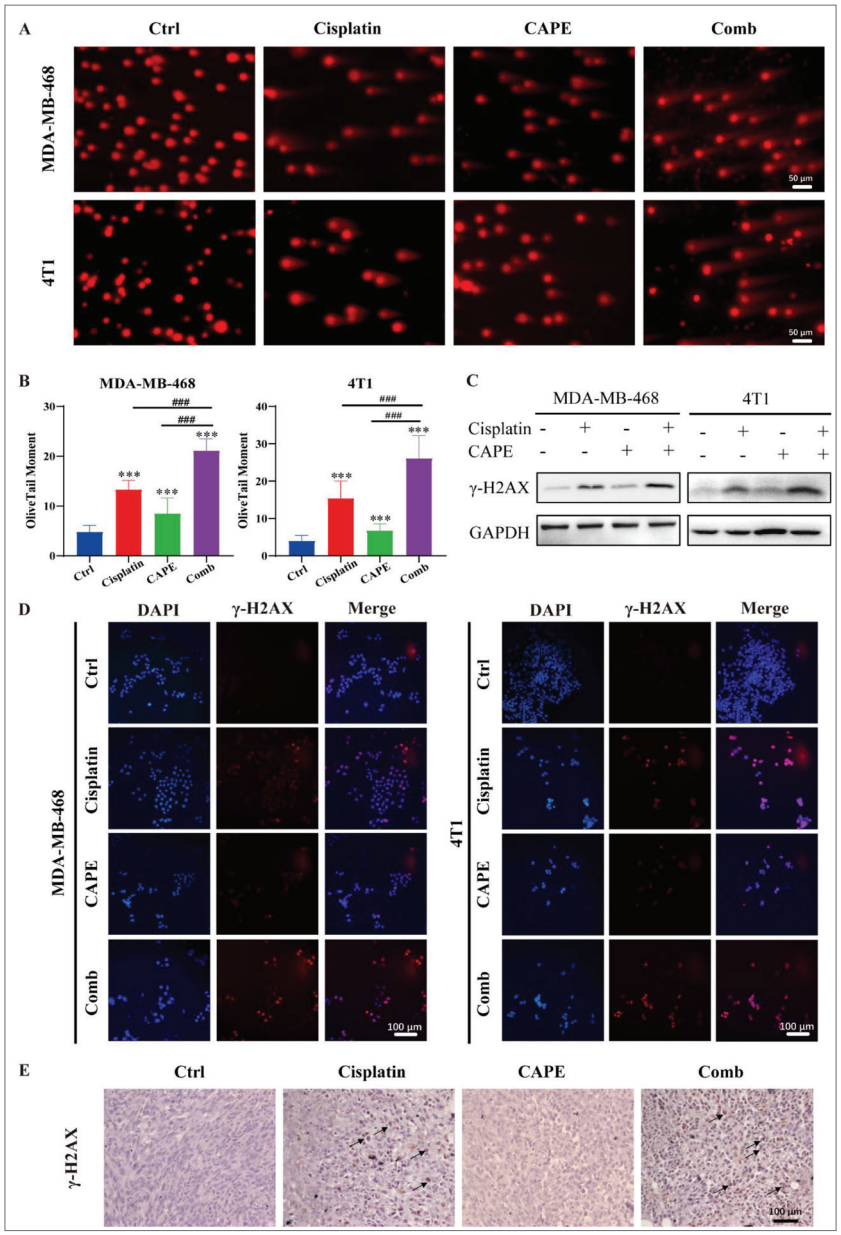

Fig. 4. CAPE enhances cisplatin-induced DNA damage in TNBC cells. **A, B –** Images and data statistics of cisplatin, CAPE monotherapy, or combined treatment induced DNA damage in MDA-MB-468 and 4T1 cells were detected by comet assay. **C –** The expression of γ-H2AX (Ser-139) in MDA-MB-468 and 4T1 cells of each group was detected by Western blotting assays. **D –** Representative images of the expression of γ-H2AX in MDA-MB-468 and 4T1 cells detected by IF analysis. **E –** Representative images of the expression of γ-H2AX in tumors of each group detected by IHC analysis. Data are presented as the mean±SD. ***P<0.001 versus control group; ###P<0.001 versus combination group.

decreased in both cell lines after pretreatment with NAC (Fig. 5A and B). These results indicate that ROS overproduction contributes to DNA damage and apoptosis induced by a combination of cisplatin and CAPE.

CAPE combined with cisplatin induces the dysregulation of the MAPK signaling pathway

To systematically elucidate the synergistic mechanism of CAPE and cisplatin, we conducted network pharmacology and transcriptomics analysis. Initially, we identified 107 cisplatin targets and 81 CAPE targets from the respective databases (Fig. 6A). Subsequently, we integrated these targets and conducted pathway enrichment analysis using an online tool, identifying the top 10 enriched pathways, including trans-synaptic signaling, ADHD and autism (ASD) pathways, the calcium signaling pathway, and the MAPK signaling pathway (Fig. 6B). Hierarchical clustering of differentially expressed genes was visualized in a heat map (Supplementary Fig. 1). KEGG pathway enrichment analysis identified the MAPK signaling pathway as the most significantly modulated by the combination therapy ($P<0.05$, $log2FC > 1$). Notably, comparative transcriptomic analysis of cisplatin-treated versus control groups (Fig. 6C) demonstrated significant enrichment of differentially expressed genes in both MAPK and Rap1 signaling pathways, suggesting their pivotal roles in mediating cisplatin's therapeutic effects. As a key member of the Ras GTPase superfamily, the Rap1 signaling pathway functionally interacts with MAPK cascades by directly activating the ERK signaling axis. Transcriptomic profiling of CAPE monotherapy revealed significant enrichment in chemical carcinogenesis-DNA adduct formation pathways (Fig. 6D), a phenomenon mechanistically linked to ROS accumulation and DNA damage responses that are established modulators of MAPK signaling [30]. Importantly, the combination group exhibited concurrent enrichment in Rap1 signaling (Fig. 6E), which was closely related to the MAPK signaling pathway. Comparative analysis of differentially expressed genes between monotherapy and combination therapy groups

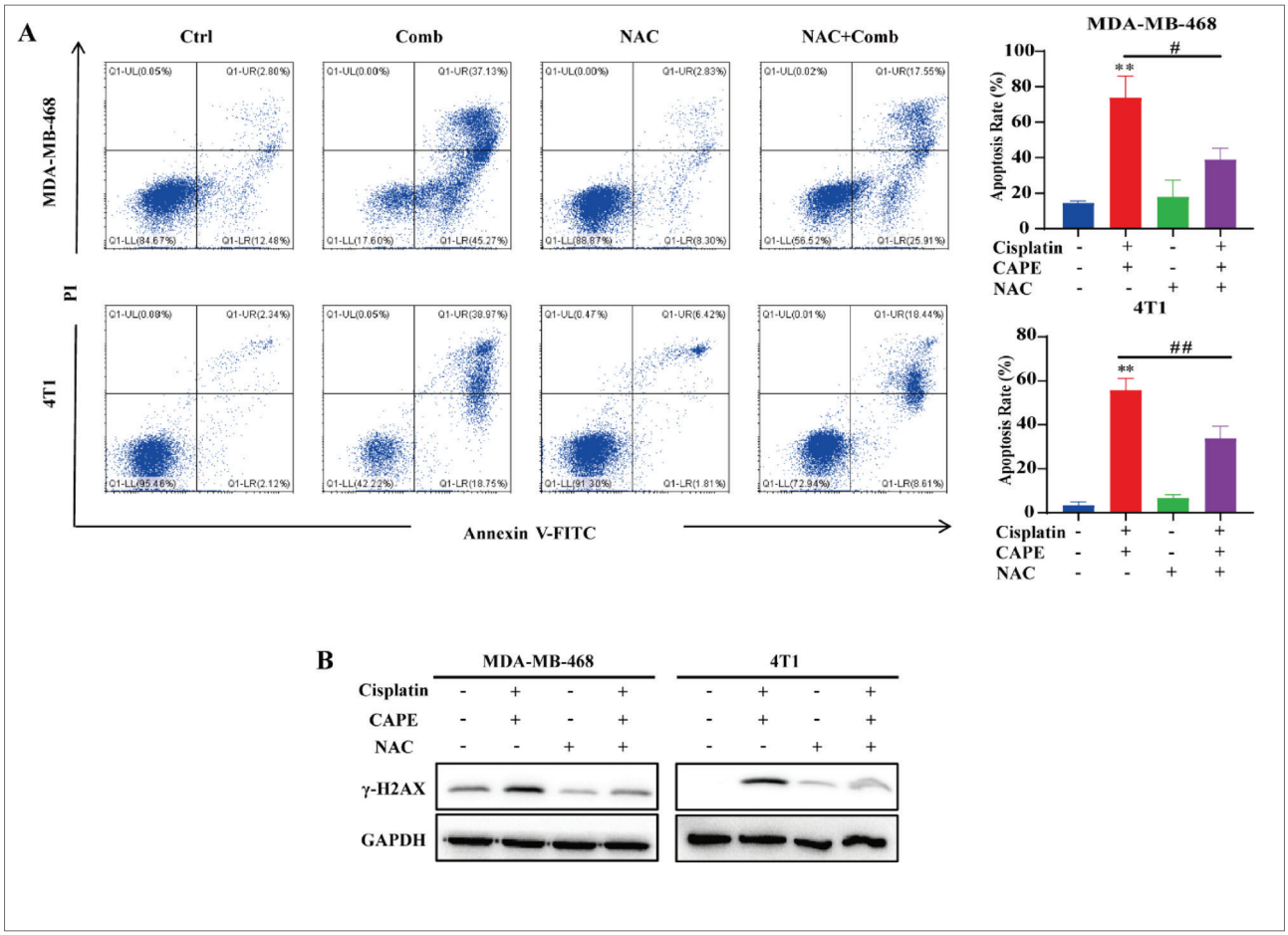

Fig. 5. NAC rescues apoptosis and DNA damage induced by co-treatment of cisplatin and CAPE in TNBC cells. **A** – MDA-MB-468 and 4T1 cells were stained with Annexin V-FITC and PI, followed by flow cytometry for cell apoptosis rate. **B** – Western blotting detected the expression of γ-H2AX in MDA-MB-468 and 4T1 cells after cisplatin, CAPE monotherapy, or combined treatment. Data are presented as the mean ± SD. $^{**}P < 0.01$ versus control group; $^{\#}P<0.05$ and $^{\#\#}P<0.01$ versus combination group.

identified 1,133 overlapping targets through Venn diagram quantification (Fig. 6F). It is noteworthy that many MAPK-related genes, such as DUSP9 and MAP2K6, are included (Fig. 6G). Thus, the integration of network pharmacology and transcriptomics analysis suggests a potential mechanism involving the MAPK signaling pathway.

To validate these findings, we assessed MAPK pathway effectors by Western blotting analysis. Consistent with transcriptomic predictions, phosphorylated p38 (p-p38) and JNK (p-JNK) levels were significantly upregulated in co-treated cells, while total protein expression remained unchanged (Fig. 7). Integrative analysis of network pharmacology, transcriptomics, and Western blotting validation demonstrates that the antitumor synergy between CAPE and cisplatin is principally mediated through coordinated regulation of the MAPK signaling axis.

DISCUSSION

Cisplatin, a conventional chemotherapeutic agent used for malignant tumors [31], has shown notable efficacy in neoadjuvant therapy and combination regimens for TNBC [32, 33]. However, the nephrotoxic effects of therapeutic-dose cisplatin restrict its clinical application and compromise treatment efficacy [34, 35]. The integration of natural compounds with chemotherapeutic agents has attracted extensive research attention in antitumor therapy, yielding promising

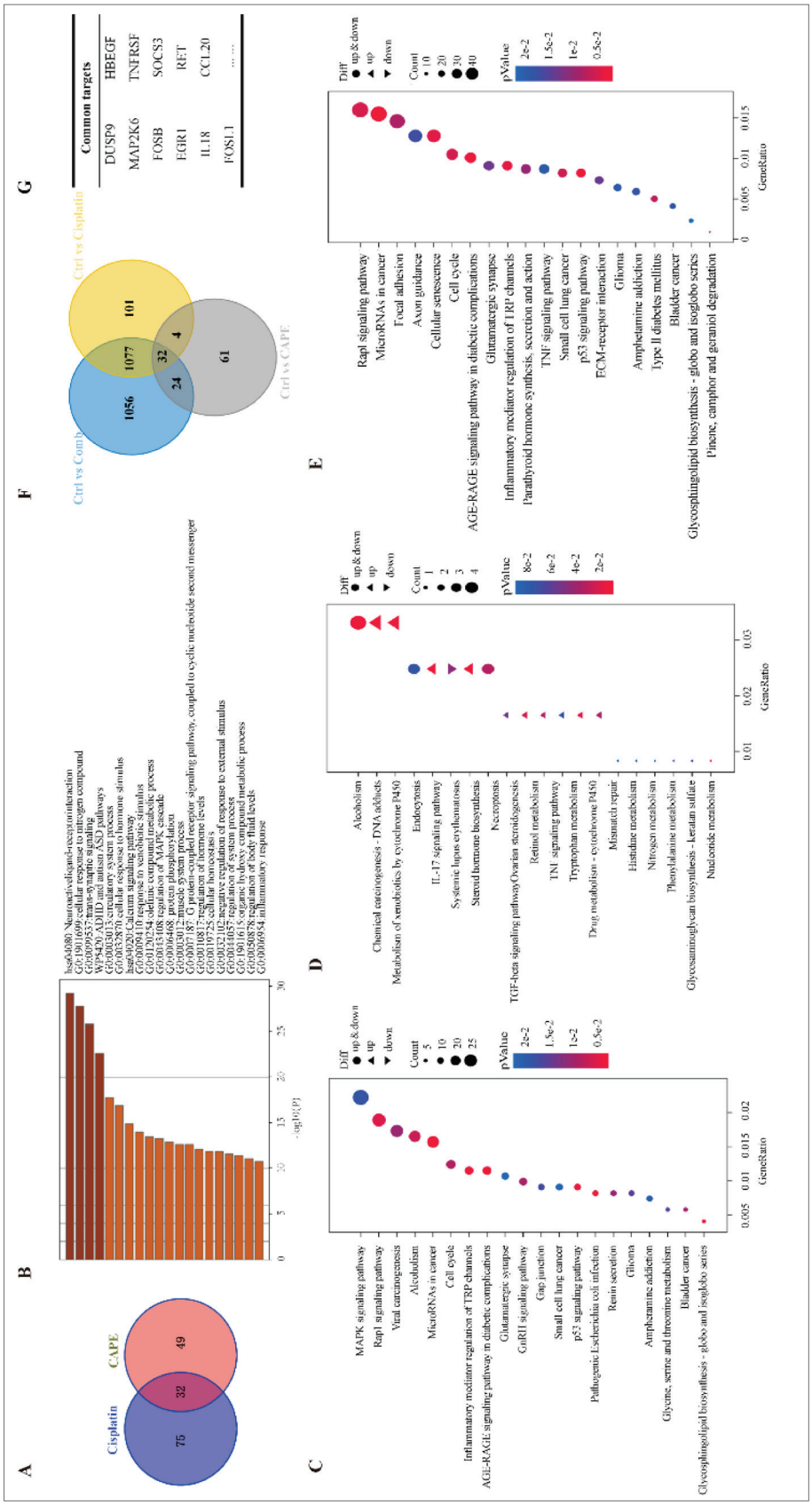

Fig. 6. Network pharmacology and transcriptomics analysis of the key pathways of cisplatin combined with CAPE on TNBC. **A** – Venn diagram analysis of cisplatin and CAPE targets on TNBC. **B** – Metascape analysis of the signaling pathways enriched in Figure 6A. **C** – KEGG enrichment analysis of differentially expressed gene in cisplatin group, **D** – CAPE group, or **E** – co-treatment group vs. control group. **F** – Venn diagram depicted the common targets of alone and co-treatment. **G** – Differentially expressed genes closely linked to the MAPK signaling pathway were identified among the screened common targets.

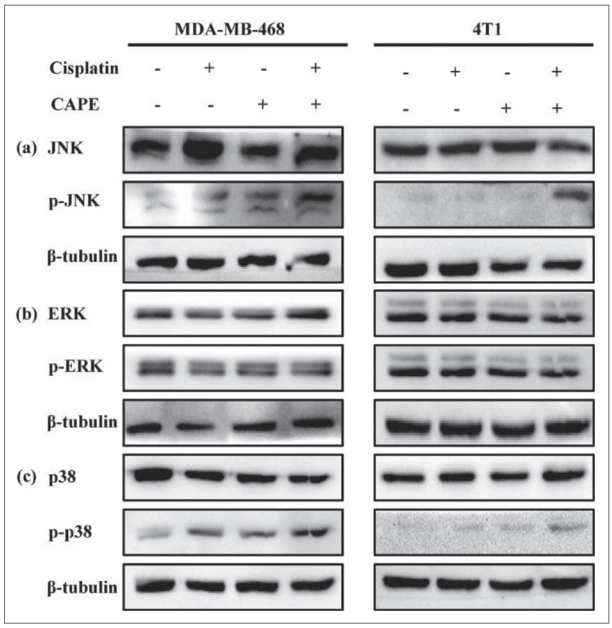

Fig. 7. Co-treatment of cisplatin and CAPE regulates the MAPK signaling pathway. The expression of (p-)JNK, (p-)p38, and (p-)ERK in MDA-MB-468 and 4T1 cells treated with cisplatin, CAPE, and co-administration was detected by western blotting.

results. Although chemotherapeutic agents are effective therapy, they often induce toxicity and adverse reactions in vital organs such as the heart, liver, and kidney. Combination with natural compounds can simultaneously mitigate these toxicities and inhibit tumor cell proliferation, thereby augmenting the antitumor effects of chemotherapy. For example, triptolide has been shown to enhance cisplatin sensitivity by conferring DNA repair in TNBC [36]. Hesperetin attenuates cisplatin-induced kidney injury by reducing oxidative stress, inflammation, and apoptosis [37]. Therefore, finding a natural compound to combine with cisplatin may be a feasible option.

Eighty percent of breast cancer patients commonly opt for alternative and natural therapies, including herbs and vitamins, to enhance survival and quality of life, indicating that herb-derived phytochemicals used alongside standard therapy may offer a promising approach [38]. Propolis, a resinous natural product produced by *Apis mellifera*, contains CAPE as its major bioactive component, which exerts diverse pharmacological effects, including anti-inflammatory, antioxidant, and antitumor activities. Previous studies have demonstrated an inhibitory effect of both propolis and CAPE on TNBC [16, 39]. However, whether CAPE can enhance the efficacy of cisplatin in TNBC remains unreported and the underlying mechanisms are worth exploring. Hence, this study aimed to investigate whether CAPE can potentiate the antitumor effect of cisplatin and also mitigate its toxic side effects.

This study demonstrated that the combination of CAPE and cisplatin exerted synergistic inhibitory effects on TNBC cell viability, as indicated by CI less than 1. Further *in vivo* experiments demonstrated that CAPE reinforced the therapeutic effect of 1 mg/kg cisplatin without compromising body weight or kidney tissue indices, with minor renal toxicity (Fig. 2). *In vivo* studies demonstrated that CAPE synergistically enhanced the antitumor efficacy of a subtherapeutic dose of cisplatin (1 mg/kg, lower than conventional dosing ranges for TNBC: 1.5-5 mg/kg) while concurrently mitigating cisplatin-induced nephrotoxicity [40-43]. To elucidate the synergistic antitumor mechanism, the MTT assay was conducted with various inhibitors. Notably, Z-VAD-FMK and NAC significantly restored cell viability, as further confirmed by induced apoptosis and ROS accumulation detected via flow cytometry, along with increased levels of cleaved caspase-3 observed through Western blotting (Fig. 3). These results suggest that the co-treatment of cisplatin and CAPE could induce more significant apoptosis and ROS overproduction than monotherapy. Additionally, the increased DNA double-strand break (DSB) detected by comet assay and the upregulated expression level of γ-H2AX (Ser-139) analyzed by Western blotting, IF, and IHC, suggest that CAPE could enhance DNA damage induced by cisplatin both *in vitro* and *in vivo*.

However, the relationship between ROS accumulation, apoptosis, and DNA damage needs further confirmation. Previous reports found that ROS triggered apoptosis through oxidizing polyunsaturated fatty acids (PUFAs) and released cytochrome C to activate caspase 3 [44]. Recent studies have demonstrated that ROS could affect DNA damage induced by genotoxic therapy such as chemotherapeutics agents [45]. Our experimental data demonstrate a causal relationship among ROS accumulation, apoptosis induction, and DNA damage, as evidenced by the ability of NAC to significantly attenuate both apoptotic cell death and γ-H2AX expression (a molecular marker of DNA

DSBs) induced by the combined treatment. This pharmacological intervention confirms the central role of oxidative stress in mediating the cytotoxic effects of the co-treatment regimen.

Network pharmacology, transcriptomics, and Western blotting revealed that the synergistic anti-TNBC mechanism of cisplatin and CAPE involves, at least in part, modulation of the MAPK signaling pathway. The results of transcriptomics analysis showed that differentially expressed genes were predominantly enriched in the MAPK signaling pathways. DUSP9, a dual-specificity phosphatase family member, functions as a negative regulator of ERK/p38 MAPK phosphorylation critical for cellular differentiation and metabolic homeostasis [46]. MAP2K6 acts as the primary upstream kinase governing p38 MAPK activation in response to cellular stress and inflammatory stimuli, thereby modulating apoptotic signaling [47].

ROS has been shown to induce apoptosis by activating the JNK and p38 pathways, whereas p-ERK1/2 supports cell survival. Notably, co-treatment with cisplatin and CAPE increased p-JNK and p-p38 levels without significantly affecting p-ERK1/2. Consistent with previous reports, our findings suggest that the combination therapy failed to activate pro-survival signaling pathways, which may explain its failure to promote cell survival. Emerging evidence highlights that multiple antitumor agents mediate their anticancer activity, at least in part, through activation of the p38 and JNK stress-activated signaling pathways. For instance, 3-deoxyappanchalcone exhibits potent pro-apoptotic effects in human esophageal cancer cells by triggering ROS-dependent activation of the JNK/p38 MAPK cascade [48]. Similarly, securinine induces programmed cell death in bladder cancer cells through selective modulation of both p38 and JNK signaling axes [49]. These findings underscore the therapeutic potential of pharmacological targeting of stress-responsive MAPK pathways to enhance tumor cell apoptosis across diverse malignancies. In addition, previous literature has reported that activation of the MAPK signaling pathway facilitates the sensitization of chemotherapeutic agents, including cisplatin and doxorubicin [50-52].

Prior research established CAPE as a USP8 inhibitor that synergizes with cisplatin to overcome chemoresistance in ovarian cancer [17]. We have now demonstrated CAPE's therapeutic efficacy in TNBC. Importantly, CAPE enhances cisplatin's antitumor effects in TNBC while reducing nephrotoxicity. This toxicity-sparing effect addresses a key clinical challenge that cisplatin-induced renal toxicity often disrupts TNBC treatment regimens. However, the molecular mechanisms of this synergy and nephroprotection require further investigation.

CONCLUSIONS

The combination of CAPE and cisplatin shows synergistic inhibitory effects against TNBC both *in vivo* and *in vitro*, as well as attenuation of cisplatin-induced nephrotoxicity. The underlying mechanisms may be mediated through enhancing ROS-induced cell apoptosis, DNA damage, and dysregulation of the MAPK signaling pathway. This study not only proposes a novel therapeutic strategy for TNBC but also highlights the potential of combination therapies through integrating chemotherapeutic agents with traditional Chinese medicine, providing valuable insights for future translational research.

Funding: This work was supported by the Key Research Project of Traditional Chinese Medicine in Zhejiang Province under Grant No. 2022ZZ008; The innovation and entrepreneurship training program of Zhejiang Students under Grant 202410344014; and the Natural Science Foundation of Zhejiang Province under Grant LY24H290002.

Acknowledgments: We appreciate the great help/technical support/experimental support from Pharmaceutical Research Center, Academy of Chinese Medical Sciences, Zhejiang Chinese Medical University.

Author contributions: Luyi Xi conducted the experiments, analyzed the data, and wrote the original draft. Yuyue Yao, Ying Lu, and Hongtao Hu performed the experiments and analyzed the data. Huajun Zhao conceived and designed the study, revised the manuscript and provided funding. All authors have read and approved the manuscript. Luyi Xi and Yuyue Yao contributed equally to this work.

Conflict of interest disclosure: The authors have no relevant financial or non-financial interests to disclose.

Data availability: The raw data underlying this article is available as an online supplementary research dataset: https://www.serbiosoc.org.rs/NewUploads/Uploads/Xi%20et%20al_Dataset.pdf

REFERENCES

1. Siegel RL, Kratzer TB, Giaquinto AN, Sung H, Jemal A. Cancer statistics, 2025. CA Cancer J Clin. 2025;75(1):10-45. https://doi.org/10.3322/caac.21871
2. Filho AM, Laversanne M, Ferlay J, Colombet M, Piñeros M, Znaor A, Parkin DM, Soerjomataram I, Bray F. The GLOBOCAN 2022 cancer estimates: Data sources, methods, and a snapshot of the cancer burden worldwide. Int J Cancer. 2024. https://doi.org/10.1002/ijc.35278
3. Meirelles LEF, Souza MVF, Carobeli LR, Morelli F, Mari NL, Damke E, Shinobu Mesquita CS, Teixeira JJV, Consolaro MEL, Silva V. Combination of Conventional Drugs with Biocompounds Derived from Cinnamic Acid: A Promising Option for Breast Cancer Therapy. Biomedicines. 2023;11(2). https://doi.org/10.3390/biomedicines11020275
4. Prat A, Pineda E, Adamo B, Galván P, Fernández A, Gaba L, Díez M, Viladot M, Arance A, Muñoz M. Clinical implications of the intrinsic molecular subtypes of breast cancer. Breast. 2015;24 Suppl 2:S26-35. https://doi.org/10.1016/j.breast.2015.07.008
5. Bou Zerdan M, Ghorayeb T, Saliba F, Allam S, Bou Zerdan M, Yaghi M, Bilani N, Jaafar R, Nahleh Z. Triple Negative Breast Cancer: Updates on Classification and Treatment in 2021. Cancers (Basel). 2022;14(5). https://doi.org/10.3390/cancers14051253
6. Leon-Ferre RA, Goetz MP. Advances in systemic therapies for triple negative breast cancer. Bmj. 2023;381:e071674. https://doi.org/10.1136/bmj-2022-071674
7. Zagami P, Carey LA. Triple negative breast cancer: Pitfalls and progress. NPJ Breast Cancer. 2022;8(1):95. https://doi.org/10.1038/s41523-022-00468-0
8. Jin J, Tao Z, Cao J, Li T, Hu X. DNA damage response inhibitors: An avenue for TNBC treatment. Biochim Biophys Acta Rev Cancer. 2021;1875(2):188521. https://doi.org/10.1016/j.bbcan.2021.188521
9. Telli ML, Timms KM, Reid J, Hennessy B, Mills GB, Jensen KC, Szallasi Z, Barry WT, Winer EP, Tung NM, Isakoff SJ, Ryan PD, Greene-Colozzi A, Gutin A, Sangale Z, Iliev D, Neff C, Abkevich V, Jones JT, Lanchbury JS, Hartman AR, Garber JE, Ford JM, Silver DP, Richardson AL. Homologous Recombination Deficiency (HRD) Score Predicts Response to Platinum-Containing Neoadjuvant Chemotherapy in Patients with Triple-Negative Breast Cancer. Clin Cancer Res. 2016;22(15):3764-73. https://doi.org/10.1158/1078-0432.CCR-15-2477
10. Hu XC, Zhang J, Xu BH, Cai L, Ragaz J, Wang ZH, Wang BY, Teng YE, Tong ZS, Pan YY, Yin YM, Wu CP, Jiang ZF, Wang XJ, Lou GY, Liu DG, Feng JF, Luo JF, Sun K, Gu YJ, Wu J, Shao ZM. Cisplatin plus gemcitabine versus paclitaxel plus gemcitabine as first-line therapy for metastatic triple-negative breast cancer (CBCSG006): a randomised, open-label, multicentre, phase 3 trial. Lancet Oncol. 2015;16(4):436-46. https://doi.org/10.1016/S1470-2045(15)70064-1
11. Ghosh S. Cisplatin: The first metal based anticancer drug. Bioorg Chem. 2019;88:102925. https://doi.org/10.1016/j.bioorg.2019.102925
12. Pabla N, Dong Z. Cisplatin nephrotoxicity: mechanisms and renoprotective strategies. Kidney Int. 2008;73(9):994-1007. https://doi.org/10.1038/sj.ki.5002786
13. Wang X, Li J, Chen R, Li T, Chen M. Active Ingredients from Chinese Medicine for Combination Cancer Therapy. Int J Biol Sci. 2023;19(11):3499-525. https://doi.org/10.7150/ijbs.77720
14. Li K, Li J, Li Z, Men L, Zuo H, Gong X. Cisplatin-based combination therapies: Their efficacy with a focus on ginsenosides co-administration. Pharmacol Res. 2024;203:107175. https://doi.org/10.1016/j.phrs.2024.107175
15. Burdock GA. Review of the biological properties and toxicity of bee propolis (propolis). Food Chem Toxicol. 1998;36(4):347-63. https://doi.org/10.1016/S0278-6915(97)00145-2
16. Wu J, Omene C, Karkoszka J, Bosland M, Eckard J, Klein CB, Frenkel K. Caffeic acid phenethyl ester (CAPE), derived from a honeybee product propolis, exhibits a diversity of anti-tumor effects in pre-clinical models of human breast cancer. Cancer Lett. 2011;308(1):43-53. https://doi.org/10.1016/j.canlet.2011.04.012
17. Colombo D, Gatti L, Sjöstrand L, Carenini N, Costantino M, Corna E, Arrighetti N, Zuccolo M, De Cesare M, Linder S, D'Arcy P, Perego P. Caffeic acid phenethyl ester targets ubiquitin-specific protease 8 and synergizes with cisplatin in endometrioid ovarian carcinoma cells. Biochem Pharmacol. 2022;197:114900. https://doi.org/10.1016/j.bcp.2021.114900
18. Tolba MF, Omar HA, Azab SS, Khalifa AE, Abdel-Naim AB, Abdel-Rahman SZ. Caffeic Acid Phenethyl Ester: A Review of Its Antioxidant Activity, Protective Effects against Ischemia-reperfusion Injury and Drug Adverse Reactions. Crit Rev Food Sci Nutr. 2016;56(13):2183-90. https://doi.org/10.1080/10408398.2013.821967
19. Albukhari AA, Gashlan HM, El-Beshbishy HA, Nagy AA, Abdel-Naim AB. Caffeic acid phenethyl ester protects against tamoxifen-induced hepatotoxicity in rats. Food Chem Toxicol. 2009;47(7):1689-95. https://doi.org/10.1016/j.fct.2009.04.021
20. Zhang Y, Kong D, Han H, Cao Y, Zhu H, Cui G. Caffeic acid phenethyl ester protects against doxorubicin-induced cardiotoxicity and increases chemotherapeutic efficacy by regulating the unfolded protein response. Food Chem Toxicol. 2022;159:112770. https://doi.org/10.1016/j.fct.2021.112770
21. Ozen S, Akyol O, Iraz M, Söğüt S, Ozuğurlu F, Ozyurt H, Odaci E, Yildirim Z. Role of caffeic acid phenethyl ester, an active component of propolis, against cisplatin-induced nephrotoxicity in rats. J Appl Toxicol. 2004;24(1):27-35. https://doi.org/10.1002/jat.941
22. Zhu Z, Shen W, Tian S, Yang B, Zhao H. F3, a novel active fraction of Valeriana jatamansi Jones induces cell death via DNA damage in human breast cancer cells. Phytomedicine. 2019;57:245-54. https://doi.org/10.1016/j.phymed.2018.12.041
23. Zhu ZH, Xu XT, Shen CJ, Yuan JT, Lou SY, Ma XL, Chen X, Yang B, Zhao HJ. A novel sesquiterpene lactone fraction from Eupatorium chinense L. suppresses hepatocellular carcinoma growth by triggering ferritinophagy and mitochondrial damage. Phytomedicine. 2023;112:154671. https://doi.org/10.1016/j.phymed.2023.154671

24. Nickel J, Gohlke BO, Erehman J, Banerjee P, Rong WW, Goede A, Dunkel M, Preissner R. SuperPred: update on drug classification and target prediction. Nucleic Acids Res. 2014;42:W26-31. https://doi.org/10.1093/nar/gku477
25. Ke H, Wang X, Zhou Z, Ai W, Wu Z, Zhang Y. Effect of weimaining on apoptosis and Caspase-3 expression in a breast cancer mouse model. J Ethnopharmacol. 2021;264:113363. https://doi.org/10.1016/j.jep.2020.113363
26. Damarla M, Parniani AR, Johnston L, Maredia H, Serebreni L, Hamdan O, Sidhaye VK, Shimoda LA, Myers AC, Crow MT, Schmidt EP, Machamer CE, Gaestel M, Rane MJ, Kolb TM, Kim BS, Damico RL, Hassoun PM. Mitogen-activated protein kinase-activated protein kinase 2 mediates apoptosis during lung vascular permeability by regulating movement of cleaved caspase 3. Am J Respir Cell Mol Biol. 2014;50(5):932-41. https://doi.org/10.1165/rcmb.2013-0361OC
27. Wu T, Liu W, Chen H, Hou L, Ren W, Zhang L, Hu J, Chen H, Chen C. Toxoflavin analog D43 exerts antiproliferative effects on breast cancer by inducing ROS-mediated apoptosis and DNA damage. Sci Rep. 2024;14(1):4008. https://doi.org/10.1038/s41598-024-53843-1
28. Kumar K, Mishra JPN, Singh RP. Usnic acid induces apoptosis in human gastric cancer cells through ROS generation and DNA damage and causes up-regulation of DNA-PKcs and γ-H2A.X phosphorylation. Chem Biol Interact. 2020;315:108898. https://doi.org/10.1016/j.cbi.2019.108898
29. Li R, Kato H, Fumimoto C, Nakamura Y, Yoshimura K, Minagawa E, Omatsu K, Ogata C, Taguchi Y, Umeda M. Essential Amino Acid Starvation-Induced Oxidative Stress Causes DNA Damage and Apoptosis in Murine Osteoblast-like Cells. Int J Mol Sci. 2023;24(20). https://doi.org/10.3390/ijms242015314
30. Rezatabar S, Karimian A, Rameshknia V, Parsian H, Majidinia M, Kopi TA, Bishayee A, Sadeghinia A, Yousefi M, Monirialamdari M, Yousefi B. RAS/MAPK signaling functions in oxidative stress, DNA damage response and cancer progression. J Cell Physiol. 2019;234(9):14951-65. https://doi.org/10.1002/jcp.28334
31. Thakur B, Ray P. Cisplatin triggers cancer stem cell enrichment in platinum-resistant cells through NF-κB-TNFα-PIK3CA loop. J Exp Clin Cancer Res. 2017;36(1):164. https://doi.org/10.1186/s13046-017-0636-8
32. Zhu Y, Hu Y, Tang C, Guan X, Zhang W. Platinum-based systematic therapy in triple-negative breast cancer. Biochim Biophys Acta Rev Cancer. 2022;1877(1):188678. https://doi.org/10.1016/j.bbcan.2022.188678
33. Dasari S, Njiki S, Mbemi A, Yedjou CG, Tchounwou PB. Pharmacological Effects of Cisplatin Combination with Natural Products in Cancer Chemotherapy. Int J Mol Sci. 2022;23(3). https://doi.org/10.3390/ijms23031532
34. Volarevic V, Djokovic B, Jankovic MG, Harrell CR, Fellabaum C, Djonov V, Arsenijevic N. Molecular mechanisms of cisplatin-induced nephrotoxicity: a balance on the knife edge between renoprotection and tumor toxicity. J Biomed Sci. 2019;26(1):25. https://doi.org/10.1186/s12929-019-0518-9
35. Blachley JD, Hill JB. Renal and electrolyte disturbances associated with cisplatin. Ann Intern Med. 1981;95(5):628-32. https://doi.org/10.7326/0003-4819-95-5-628
36. Zhang Z, Sun C, Zhang L, Chi X, Ji J, Gao X, Wang Y, Zhao Z, Liu L, Cao X, Yang Y, Mao W. Triptolide interferes with XRCC1/PARP1-mediated DNA repair and confers sensitization of triple-negative breast cancer cells to cisplatin. Biomed Pharmacother. 2019;109:1541-6. https://doi.org/10.1016/j.biopha.2018.11.008
37. Chen X, Wei W, Li Y, Huang J, Ci X. Hesperetin relieves cisplatin-induced acute kidney injury by mitigating oxidative stress, inflammation and apoptosis. Chem Biol Interact. 2019;308:269-78. https://doi.org/10.1016/j.cbi.2019.05.040
38. Pradeep Prabhu P, Mohanty B, Lobo CL, Balusamy SR, Shetty A, Perumalsamy H, Mahadev M, Mijakovic I, Dubey A, Singh P. Harnessing the nutriceutics in early-stage breast cancer: mechanisms, combinational therapy, and drug delivery. J Nanobiotechnology. 2024;22(1):574. https://doi.org/10.1186/s12951-024-02815-8
39. Rzepecka-Stojko A, Kabała-Dzik A, Moździerz A, Kubina R, Wojtyczka RD, Stojko R, Dziedzic A, Jastrzębska-Stojko Ż, Jurzak M, Buszman E, Stojko J. Caffeic Acid phenethyl ester and ethanol extract of propolis induce the complementary cytotoxic effect on triple-negative breast cancer cell lines. Molecules. 2015;20(5):9242-62. https://doi.org/10.3390/molecules20059242
40. Lee JO, Kang MJ, Byun WS, Kim SA, Seo IH, Han JA, Moon JW, Kim JH, Kim SJ, Lee EJ, In Park S, Park SH, Kim HS. Metformin overcomes resistance to cisplatin in triple-negative breast cancer (TNBC) cells by targeting RAD51. Breast Cancer Res. 2019;21(1):115. https://doi.org/10.1186/s13058-019-1204-2
41. Tian C, Wei Y, Li J, Huang Z, Wang Q, Lin Y, Lv X, Chen Y, Fan Y, Sun P, Xiang R, Chang A, Yang S. A Novel CDK4/6 and PARP Dual Inhibitor ZC-22 Effectively Suppresses Tumor Growth and Improves the Response to Cisplatin Treatment in Breast and Ovarian Cancer. Int J Mol Sci. 2022;23(5). https://doi.org/10.3390/ijms23052892
42. Islam SS, Al-Sharif I, Sultan A, Al-Mazrou A, Remmal A, Aboussekhra A. Eugenol potentiates cisplatin anti-cancer activity through inhibition of ALDH-positive breast cancer stem cells and the NF-κB signaling pathway. Mol Carcinog. 2018;57(3):333-46. https://doi.org/10.1002/mc.22758
43. Huang Y, Wu H, Li X. Novel sequential treatment with palbociclib enhances the effect of cisplatin in RB-proficient triple-negative breast cancer. Cancer Cell Int. 2020;20:501. https://doi.org/10.1186/s12935-020-01597-x
44. Wang B, Wang Y, Zhang J, Hu C, Jiang J, Li Y, Peng Z. ROS-induced lipid peroxidation modulates cell death outcome: mechanisms behind apoptosis, autophagy, and ferroptosis. Arch Toxicol. 2023;97(6):1439-51. https://doi.org/10.1007/s00204-023-03476-6
45. Srinivas US, Tan BWQ, Vellayappan BA, Jeyasekharan AD. ROS and the DNA damage response in cancer. Redox Biol. 2019;25:101084. https://doi.org/10.1016/j.redox.2018.101084
46. Keyse SM. Dual-specificity MAP kinase phosphatases (MKPs) and cancer. Cancer Metastasis Rev. 2008;27(2):253-61. https://doi.org/10.1007/s10555-008-9123-1

47. Juyoux P, Galdadas I, Gobbo D, von Velsen J, Pelosse M, Tully M, Vadas O, Gervasio FL, Pellegrini E, Bowler MW. Architecture of the MKK6-p38α complex defines the basis of MAPK specificity and activation. Science. 2023;381(6663):1217-25. https://doi.org/10.1126/science.add7859
48. Kwak AW, Lee MJ, Lee MH, Yoon G, Cho SS, Chae JI, Shim JH. The 3-deoxysappanchalcone induces ROS-mediated apoptosis and cell cycle arrest via JNK/p38 MAPKs signaling pathway in human esophageal cancer cells. Phytomedicine. 2021;86:153564. https://doi.org/10.1016/j.phymed.2021.153564
49. Xie L, Liang S, Jiwa H, Zhang L, Lu Q, Wang X, Luo L, Xia H, Li Z, Wang J, Luo X, Luo J. Securinine inhibits the tumor growth of human bladder cancer cells by suppressing Wnt/β-catenin signaling pathway and activating p38 and JNK signaling pathways. Biochem Pharmacol. 2024;223:116125. https://doi.org/10.1016/j.bcp.2024.116125
50. Hankittichai P, Thaklaewphan P, Wikan N, Ruttanapattanakul J, Potikanond S, Smith DR, Nimlamool W. Resveratrol Enhances Cytotoxic Effects of Cisplatin by Inducing Cell Cycle Arrest and Apoptosis in Ovarian Adenocarcinoma SKOV-3 Cells through Activating the p38 MAPK and Suppressing AKT. Pharmaceuticals (Basel). 2023;16(5). https://doi.org/10.3390/ph16050755
51. Wei T, Xiaojun X, Peilong C. Magnoflorine improves sensitivity to doxorubicin (DOX) of breast cancer cells via inducing apoptosis and autophagy through AKT/mTOR and p38 signaling pathways. Biomed Pharmacother. 2020;121:109139. https://doi.org/10.1016/j.biopha.2019.109139
52. Jiang XY, Zhu XS, Xu HY, Zhao ZX, Li SY, Li SZ, Cai JH, Cao JM. Diallyl trisulfide suppresses tumor growth through the attenuation of Nrf2/Akt and activation of p38/JNK and potentiates cisplatin efficacy in gastric cancer treatment. Acta Pharmacol Sin. 2017;38(7):1048-58. https://doi.org/10.1038/aps.2016.176

ONLINE SUPPLEMENTARY RESEARCH DATASET

Supplementary Fig. S1. Heatmap analysis showed differentially expressed genes in the cisplatin, CAPE, and co-treatment groups vs the control groups.

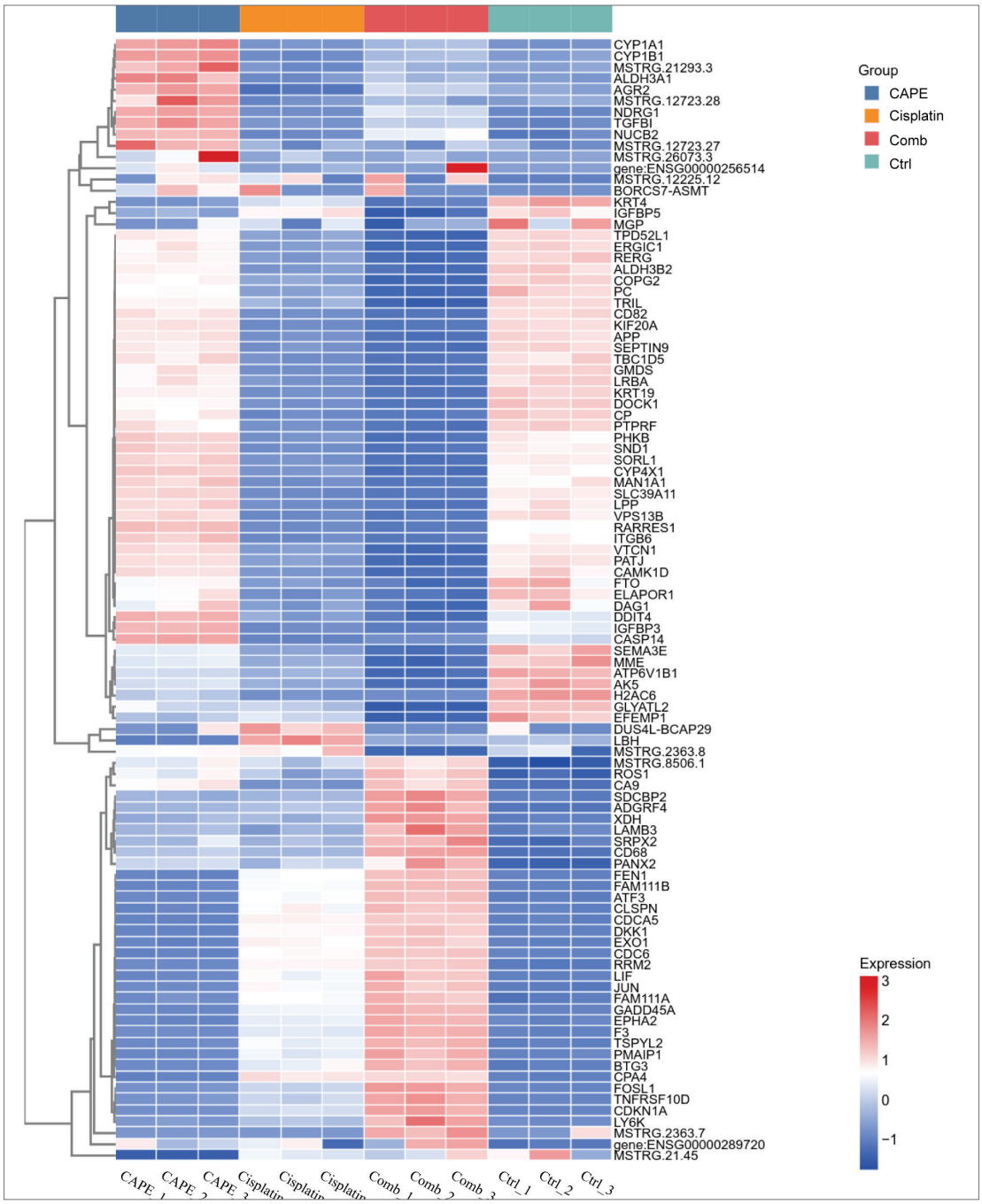

RESEARCH DATASET

The raw data underlying this article is available as an online supplementary research dataset:
https://www.serbiosoc.org.rs/NewUploads/Uploads/Xi%20et%20al_Dataset.pdf